Food Hydrocolloids 122 (2022) 107075

Contents lists available at ScienceDirect

Food Hydrocolloids

journal homepage: www.elsevier.com/locate/foodhyd

pH influences the interfacial properties of blue whiting (*M. poutassou*) and whey protein hydrolysates determining the physical stability of fish oil-in-water emulsions

José María Ruiz-Álvarez [a], Teresa del Castillo-Santaella [b], Julia Maldonado-Valderrama [b,c], Antonio Guadix [a], Emilia M. Guadix [a], Pedro J. García-Moreno [a,*]

[a] Department of Chemical Engineering, University of Granada, Granada, Spain
[b] Department of Applied Physics, University of Granada, Granada, Spain
[c] Excellence Research Unit "Modeling Nature" (MNat), University of Granada, Granada, Spain

ARTICLE INFO

Keywords:
Fish oil-in-water emulsions
Protein hydrolysates
Emulsifier peptides
Interfacial tension
Interfacial dilatational rheology
Physical stability

ABSTRACT

This work investigates the influence of the interfacial properties of whey protein (WPH) and blue whiting protein (BPH) hydrolysates on the physical stability of fish oil-in-water emulsions stabilized with these hydrolysates at pH 2 or 8. Measurements of interfacial tension and dilatational rheology confirmed that pH is a key factor affecting these interfacial properties of WPH and BPH. WPH, when tested at 1 and 10 mg/mL, showed a higher interfacial activity at pH 8 when compared to pH 2 or to BPH at pH 8 or 2, despite having a lower protein content. Moreover, when tested at 0.1 and 1 mg/mL, the dilatational modulus of WPH was significantly higher at pH 8 than at pH 2. These findings correlate with the formation of smaller oil droplets and a more resistant interfacial peptide layer for WPH at pH 8, hence explaining the improved physical stability of the 5% fish oil-in-water emulsion stabilized with WPH at pH 8. BPH did not show significant differences in interfacial activity with pH but exhibited significantly higher dilatational elasticity and viscosity at pH 2 compared to pH 8 (when measured at 0.1 mg/mL and 0.01 or 0.1 Hz). This correlates with the formation of stable 5% fish oil-in-water emulsions with BPH at pH 2 but not at pH 8.

1. Introduction

Fish oil, compared to other animal and vegetable oils, presents a high content of long chain omega-3 polyunsaturated fatty acids (omega-3 PUFA), which include eicosapentaenoic (EPA 20:5n-3) and docosahexaenoic (DHA, 22:6n-3) acids (Bimbo, 2013). Omega-3 PUFA have been scientifically reported to promote numerous beneficial effects in human health, such as prevention of cardiovascular diseases, reduction of the symptoms in rheumatoid arthritis or prevention of some types of cancer (Belury, 2002; Elagizi et al., 2018; Shahidi, 2015). Furthermore, some studies report positive effects of omega-3 PUFA in the treatment of mental diseases such as depression or schizophrenia (Schram et al., 2007), and also a relevant importance in the brain, eye and nervous system development in infants, children, and maternal healthy (Arab-Tehrany et al., 2012; Shahidi & Ambigaipalan, 2018). Currently, the benefits of omega-3 PUFA administration in COVID-19 patients have been investigated in various studies owing to its implication in the cytokines storm developed by the disease (Arnardottir et al., 2021; Vivar-Sierra et al., 2021; Weill, Plissonneau, Legrand, Rioux, & Thibault, 2020).

Humans are able to synthesize EPA and DHA from α-linolenic acid (ALA, C18:3n-3) through desaturation and elongation reactions. Nevertheless, this conversion is limited (Brenna, Salem, Sinclair, & Cunnane, 2009), being necessary its intake through the diet. However, the generalized low consumption by western populations of fatty fish and food enriched with microalgae or krill, which are the principal natural sources of omega-3 PUFA, does not reach the recommended daily intakes. This fact has led to an increasingly interest by food industry in the production of food enriched with omega-3 PUFA such as milk, bread, infant formula, energy bars, hen eggs, or mayonnaise (Miguel et al., 2019; Nielsen & Jacobsen, 2009; Stupin, Rasic, Anita, Marko, & Zlata, 2018).

The high susceptibility to lipid oxidation of omega-3 PUFA is the main challenge for their incorporation into food, affecting negatively to

* Corresponding author.
E-mail address: pjgarcia@ugr.es (P.J. García-Moreno).

https://doi.org/10.1016/j.foodhyd.2021.107075
Received 4 April 2021; Received in revised form 27 July 2021; Accepted 29 July 2021
Available online 30 July 2021

the product quality (e.g. odour, flavour and loss of nutritive value) (Berton-Carabin, Ropers, & Genot, 2014). Thus, food industry has developed delivery systems such as fish oil-in-water emulsions, that, when well designed, allow to successfully disperse omega-3 PUFA within the food matrix and reduce lipid oxidation. Indeed, the existence of a protective and charged interfacial physical barrier in fish oil-in-water emulsions might lead to a reduction in possible interactions between the oil and prooxidants (i.e., oxygen, radicals, metal ions) (García-Moreno, Guadix, Guadix, & Jacobsen, 2016). However, oil-in-water emulsions are thermodynamically unstable systems, being necessary to add emulsifiers in order to obtain physically stable emulsions during a desired time. Proteins are common emulsifiers, used by food industry for the production of omega-3 delivery emulsions, since they are natural ingredients, which may also exhibit antioxidant properties (i.e., radical scavenging or chelating activities) (Berton-Carabin et al., 2014).

Protein emulsifiers are amphiphilic molecules which interact with the aqueous and oleic phases. This interaction causes: i) a reduction in interfacial tension and free energy of the system, favouring emulsion formation (i.e, oil droplets disruption) (Maldonado-Valderrama, 2006), and ii) an enhanced physical stability of the emulsion by minimizing flocculation and preventing coalescence due to steric and electrostatic repulsions provided by the protein interfacial layer (Berton-Carabin et al., 2014).

In particular, the interfacial properties of emulsions such as interfacial tension, interfacial elasticity and viscosity have been reported as key parameters determining the physical stability of protein-stabilized emulsions in foods (Aguilera-Garrido, del Castillo-Santaella, Galisteo--González, JoséGálvez-Ruiz, & Maldonado-Valderrama, 2021; Maldonado-Valderrama et al., 2008; Aguilera-Garrido et al., 2021; Carrera Sánchez & Rodríguez Patino, 2021; Del Castillo-Santaella, Sanmartín, Cabrerizo-Vílchez, Arboleya, & Maldonado-Valderrama, 2014; Felix, Romero, Carrera-sanchez, & Guerrero, 2019; Maldonado-Valderrama et al., 2008; Schröder, Berton-Carabin, Venema, & Cornacchia, 2017; Torcello-Gómez, Maldonado-Valderrama, Jódar-Reyes, & Foster, 2013). In this regard, functional properties of proteins, such as emulsifying and antioxidant capacity, can be improved by enzymatic hydrolysis of proteins, when using the right enzyme and achieving an optimum degree of hydrolysis (DH) (Carrera Sánchez & Rodríguez Patino, 2021; García--Moreno et al., 2016; Padial-Domínguez, Espejo-Carpio, García-Moreno, Jacobsen, & Guadix, 2020). Hydrolysis of peptide bonds results in peptides with lower molecular weight and different structure (i.e. secondary structure) compared to the initial protein. This allows: i) a faster diffusion of peptides from the aqueous phase to the interface due to their smaller size when compared to the initial protein, and ii) an increased exposure of hydrophobic groups in peptides due to the change in structure (Rahali, Chobert, Haertlé, & Guéguen, 2000). Both properties improve peptide adsorption onto the oil/water interface, hence favouring formation and physical stability of emulsions. Nevertheless, it is worth noting that too high DH causes a major increase in the number of amine and carboxylic charged groups due to the increasing rupture of peptide bonds. This in turn, decreases the overall hydrophobicity of the resulting hydrolysate, which reduces the anchoring of peptides at the oil/water interface leading to higher interfacial tension values and in consequence lower interfacial coverage (Schröder et al., 2017). Therefore, protein hydrolysates with high emulsifying activity from different natural sources (i.e, dairy, plants and fish) are generally obtained by controlled hydrolysis, reaching low DH (i.e., DH $\leq$ 10%) (García-Moreno et al., 2016; Gbogouri, Linder, Fanni, & Parmenter, 2004; Morales-Medina, Tamm, Guadix, Guadix, & Drusch, 2016; Padial-Domínguez et al., 2020; Tamm et al., 2015).

Previous studies from our group have reported the up-grading of fishing by-products by the production of fish protein hydrolysates exhibiting emulsifying and antioxidant activities, which were successfully used to physically stabilize fish oil-in-water emulsions (García--Moreno et al., 2016; Morales-Medina et al., 2016; Padial-Domínguez et al., 2020). Curiously, fish oil-in-water emulsions stabilized with fish protein hydrolysates were only physically stable at low pH.

In the light of the above, this work aimed at investigating the effect of pH on the interfacial properties (e.g., interfacial adsorption and dilatational rheology) of blue whiting protein hydrolysate and correlate it with the physical stability of fish oil-in-water emulsions stabilized with this hydrolysate. Blue-whiting protein hydrolysate (BPH) obtained using trypsin (DH = 4%), which was recently reported to exhibit emulsifying activity (Padial-Domínguez et al., 2020), was selected for this study. In addition, and for the sake of comparison between fish and diary protein hydrolysates, we also evaluated the interfacial properties of whey protein hydrolysate (WPH) obtained by using subtilisin (DH = 10%) due to its excellent emulsifying properties (Padial-Domínguez et al., 2020). Correlating interfacial properties with emulsion formation and stability it is needed for the rational design of emulsions with improved characteristics.

2. Materials and methods

2.1. Materials

Whey protein concentrate (Wheyco GmbH, Hamburg, Germany) was used as a substrate to produce whey protein hydrolysate (WPH), employing subtilisin (EC 3.4.21.62), provided by Novozymes (Bagsvaerd, Denmark) for enzymatic hydrolysis until attaining a final DH of 10% (Padial-Domínguez et al., 2020). After completion of the hydrolysis, samples were heated to 100 °C for 15 min to deactivate the enzyme and then centrifuged to remove the remaining solids (20,000*g*, 15 min). Finally, samples were filtered under vacuum (pore size: 10 μm). The purification step was carried out twice and samples were stored at −80 °C until they were lyophilized in a Labconco freeze drying system (Kansas City, MO, USA). The proximate composition of the resulting WPH was as previously reported by Padial-Domínguez et al. (2020): protein 32.65 ± 0.78%, lipid 2.29 ± 0.01%, moisture 5.32 ± 0.17%, ash 8.08 ± 0.11%. The rest up to 100% (~51.7%) might be considered as carbohydrates. To produce blue whiting protein hydrolysate (BPH), blue whiting (*Micromesistius poutassou*) purchased from the fishing harbor of Motril (Spain) was employed as a raw material. Dewatered and defatted substrate was obtained after pressing the whole fish according to the process described elsewhere (García-Moreno, Horn, & Jacobsen, 2014). The protein cake was grinded in a Sammic cutter SK-3 (Guipúzcua, Spain) and the mix was kept at −80 °C until use. Blue whiting was hydrolysed using trypsin (EC 3.4.21.4), also provided by Novozymes, to obtain a final DH of 4% (Padial-Domínguez et al., 2020). After hydrolysis, the sample was treated as described above for WPH. The proximate composition of the resulting BPH was as previously reported by Padial-Domínguez et al. (2020): protein 76.76 ± 0.43%, lipid 9.35 ± 0.15%, moisture 3.35 ± 0.06%, ash 7.31 ± 0.08%. Refined fish oil, Omevital 18/12 TG Gold was purchased from BASF Personal Care and Nutrition GmbH (Illertissen, Germany) with a minimum content of omega-3 fatty acids of 35% (18% of EPA and 12% of DHA) and was used as received. The rest of reagents used were of analytical grade.

2.2. Preparation of emulsions

Firstly, the aqueous phase of the emulsions was prepared by dissolving each hydrolysate in Milli-Q water and adjusting their pH with HCl (1 M) or NaOH (1 M). Emulsions at pH 8 and pH 2 were prepared using WPH as emulsifier, whilst emulsions could be only stabilized with BPH at pH 2. In agreement with this, previous studies in our group have reported that fish oil-in-water emulsions stabilized with fish protein hydrolysates at pH 8 immediately separate after homogenization (Morales-Medina et al., 2016; Padial-Domínguez et al., 2020).

All emulsions were produced with an hydrolysate content of 2% w/w and 5% w/w of fish oil, following the same procedure described by Padial-Domínguez (2020). The hydrolysates were totally soluble at this

concentration. Firstly, a coarse emulsion was produced through agitation in Ultra-Turrax (IKA Werke GmbH & Co, Staufen, Germany) at 15 000 rpm for 2 min, adding fish oil in the first minute of agitation. Then the coarse emulsion was passed through a two phases homogenizer (Panda Plus 2000, GEA Niro Soavi, Lübeck, Germany) at 450 bar in the first phase and 75 bar in the second, in a total of 3 passes. Sodium azide (0.05 wt% in the emulsion) was added to prevent microbial growth. Emulsions were stored in glasses of 250 mL in an incubator at 25 °C for 7 days in the dark. Samples were taken at day 0 for zeta potential measurements and days 0, 4 and 7 for droplet size measurements.

2.3. Physical stability of emulsions

2.3.1. Zeta potential

Zeta potential was measured in a Zetasizer Nano ZS (Malvern Instruments Ltd., Worcestershire, UK) at 25 °C at day 0. Samples were previously diluted in a volume proportion 2/1000 with distilled water, adjusting their pH to 2 or 8 with HCl (1 M) and NaOH (1 M), respectively. Measurements were made in triplicate.

2.3.2. Droplet size

Droplet size was measured by laser diffraction in a Mastersizer 2000 (Malvern Instruments Ltd., Worcestershire, UK). Emulsions were diluted with water in recirculation until an obscurity of 12–15% was reached. Refraction indexes of sunflower oil (1.469) and water (1.330) were used as particle and dispersant, respectively. Results are reported as mean volume diameter ($D_{4,3}$). Measurements were made in triplicate.

2.4. Interfacial characterisation

2.4.1. Preparation of aqueous solutions

Aqueous solutions of the hydrolysates were prepared the day before measuring by dissolving the hydrolysate in ultrapure water produced through a purification Milli-Q water system (0.054 μS). Solutions were stirred (300 rpm) for 3 h, and the pH was adjusted by using either HCl (1 M) or NaOH (1 M). Solutions were stirred (300 rpm) overnight at 4 °C. Before measuring, the solutions were stirred (300 rpm) at room temperature for 30 min.

These aqueous solutions were prepared at hydrolysate concentrations of 0.001, 0.01, 0.1, 1 and 10 mg/mL at pH 2 and pH 8 for both hydrolysates. All glassware was washed with 10% Micro-90 cleaning solution and exhaustively rinsed with tap water, isopropanol, deionized water, and ultrapure water in this sequence (Del Castillo-Santaella et al., 2014). Aqueous solutions were prepared in duplicate.

2.4.2. Interfacial tension

Measurements of interfacial tension and dilatational rheology were carried out using a pendant drop tensiometer designed at the University of Granada (patent ES 2 153 296 B1/WO 2012/080536 A, ES) and fully described elsewhere (Cabrerizo-Vílchez, Wege, Holgado-Terriza, & Neumann, 1999; Maldonado-Valderrama, Torcello-Gómez, Del Castillo-Santaella, Holgado-Terriza, & Cabrerizo-Vílchez, 2015). This system is composed of 4 basic subsystems: an illumination system, an image compiler system, a flux controller and an antivibration system. The illumination system was formed by a light source and a diffusor, which was employed to obtain a uniform illumination of the drop. Image acquisition was made by a video camera CCD (Pixelink®) connected to an optical microscope (Edmund Optics®), providing digitalized images with a resolution of 1280 × 1024 pixels with 256 gray scales. Liquid flux was injected to the drop through a micro-injector, which pumped the solution into a Teflon tip with a fixed speed and an established drop volume. All the system lies on a vibration isolation table 'Kinetic System Inc. Vibraplane' to avoid the influence of any kind of vibration during the experiments. Measurements were made at room temperature (25 °C). The whole set up is computer controlled by softwares DINATEN© and CONTACTO©, also fully developed at the University of Granada. The calculation is based on Axisymmetric Drop Shape Analysis (ADSA), adjusting drop profiles to Young-Laplace capillarity equation (Eq. (1)) (Tippel, Böttcher, & Drusch, 2016) through the determination of difference pressure (ΔP) and the two principal radii of curvature of the drop (R_1 y R_2).

$$\Delta P = \gamma\left(\frac{1}{R_1}+\frac{1}{R_2}\right) \quad (1)$$

DINATEN© processes the digitized images of pendant drops and extracts the experimental drop profiles, which are fitted later to the Young-Laplace equation of capillarity by using ADSA. The program provides as outputs, the drop volume V, the interfacial tension γ, and the interfacial area A.

The pendant drop with the aqueous solution (25 μL) was formed at the end of the capillary and immersed in a glass cuvette (Hellma®) filled with fish oil simulating an oil-in-water emulsion. The adsorption process was then registered at a constant interfacial area of 39 mm^2 through a fuzzy logic algorithm PID for 3000 s (Cabrerizo-Vílchez et al., 1999). All measurements were made in duplicate for each aqueous solution of hydrolysates described above. The oil was used as received and the absence of surface active contaminants in the oil was confirmed before every measurement by checking the interfacial tension of the oil, yielding a constant value of 24.5 ± 0.2 mN/m at 20 °C. This value coincided with that obtained after purification of the oil with Florisil® resins (Fluka, 60-10 mesh, 46385) (see Fig. 1S in Supplementary Material) following the procedure used in previous works (Maldonado--Valderrama, Terriza, Torcello-Gómez, & Cabrerizo-Vílchez, 2013, Del Castillo-Santaella et al., 2014).

2.4.3. Interfacial dilatational rheology

Dilatational rheology of the interfacial films was measured applying a periodic perturbation to the interface at the end of the adsorption process. The amplitude values ranged between 3 and 3.3% A/A_0, where A is amplitude in every time and A_o is initial amplitude. This deformation provides a linear interfacial tension response (Rühs, Affolter, Windhab, & Fischer, 2013). The drop is subjected to 10 cycles of deformation at different frequencies 0.01, 0.1 and 1 Hz. Each cycle was followed by constant interfacial area monitorization for 1 min. The system records the interfacial tension response to this area deformation, using the software CONTACTO® to calculate complex interfacial dilatational modulus (E) and all related quantities (Maldonado-Valderrama et al., 2013). The complex dilatational modulus is in the general case a complex quantity given by Equation (2):

$$E = E' + iE'' = \varepsilon_d + if\eta_d \quad (2)$$

The real part corresponds to the storage modulus (E′) which matches with the interfacial dilatational elasticity (ε_d). The imaginary part corresponds to the loss modulus (E″) which is proportional to the dilatational interfacial viscosity (η_d), being 'f' the oscillatory angular frequency. E contains information about inter- and intra-molecular interactions within the adsorbed layer and can quantify the ability of the adsorbed layer to resist external disturbances and prevent the rupture of the layer (Maldonado-Valderrama et al., 2008). The relative values of the interfacial dilatational elasticity and viscosity depend on the frequency of the oscillation applied (Maldonado-Valderrama et al., 2005). Namely, when the oscillation frequency is low, the adsorbed layer has time to adapt to the deformation, allowing for relaxation process and offering low resistance to deformation (showing high surface viscosity). Conversely, when the oscillation frequency is high the adsorbed layer has no time to adapt to deformation and the system resists the compression behaving as if it was insoluble (showing high surface elasticity). Hence, at low frequencies (0.01 Hz), the surface viscosity of the adsorbed layer is maximized whereas at high frequencies the surface elasticity of the adsorbed layer prevails (0.1 Hz). Measurements were made in duplicate for each sample.

2.5. Statistical analysis

Data were subjected to analysis of variance (ANOVA) by using Statgraphics version 5.1 (Statistical Graphics Corp., Rockville, MD, USA). Tukey's multiple range test was used to determine significant differences between mean values. Differences between mean values were considered significant at a level of confidence of 95% ($p < 0.05$).

3. Results and discussion

3.1. Physical stability

The physical stability of the emulsions was evaluated during one week of storage by measuring zeta potential and droplet size. It should be noted that an oil-in-water emulsion stabilized with BPH at pH 8 was previously reported to immediately break after leaving the homogenizer (Padial-Domínguez et al., 2020), which is in accordance with previous studies that employed fish protein hydrolysates to stabilize oil-in-water emulsions (Morales-Medina et al., 2016).

3.1.1. Zeta potential

The three physically stable emulsions after production had net zeta potential values higher than ±30 mV (Table 1). Theoretically, this indicates that the electrostatic repulsions created between oil droplets are high enough to avoid physical destabilization of the emulsions by coagulation and flocculation (Maldonado-Valderrama, 2006).

As expected, WPH-stabilized emulsion at pH 8 had negative zeta potential due to the deprotonation of carboxylic groups of the peptides at pH above the pI (Table 1). The pI of WPH was determined as 4.06 ± 0.05 (see Fig. 2Sa in Supplementary Material). Schröder et al. obtained a zeta potential of −25 mV for emulsion stabilized by 0.5 wt% whey protein, a slightly higher negative zeta potential (−26 mV) for H1 (Whey protein hydrolysed, DH 5.2%) and −30 mV for H2 (Whey protein hydrolysed, DH 10%), all of them diluted in 50 mM KCl (Schröder et al., 2017). A similar value of zeta potential (−44 ± 0.6 mV) than the one obtained in this study was reported by Padial-Domínguez et al. (2020) for an emulsion stabilized with WPH at pH 8 but using 2 wt% protein (Table 1). On the contrary, WPH- and BPH-stabilized emulsions at pH 2 provided positive zeta potential values because of the protonation of the amino groups of the peptides at pH below the pI (Table 1). The pI of BPH was determined as 4.39 ± 0.01 (see Fig. 2Sb in Supplementary Material). On the other hand, differences were observed between the zeta potential of the emulsion stabilized by BPH at pH 2 in this study (54.4 ± 1.8 mV) and the results found in previous studies for emulsions stabilized at pH below pI with BPH (36.3 ± 0.1 mV) (Padial-Domínguez et al., 2020) and other fish protein hydrolysates such as horse mackerel (45.0 ± 0.1 mV) (Morales-Medina et al., 2016) and cod (30 mV) (Petursson, Decker, & McClements, 2004). These findings may be related to the different nature of the emulsifier peptides present in the different hydrolysates, to the degree of hydrolysis and to potential differences in the buffer/aqueous phase used leading to different ionic strength (Guzey, Kim, & McClements, 2004).

3.1.2. Droplet size

Emulsions stabilized with WPH did not present creaming after 7 days of storage, whilst emulsion stabilized with BPH at pH 2 presented a separated oil layer on the top at day 7. Table 1 shows the droplet size of the different emulsions during storage and Fig. 3S in Supplementary Material shows the droplet size distribution for the emulsions during storage. The three emulsions evaluated showed bimodal droplet size distribution at day 0, with peaks centred at ~0.15 and ~0.7 μm (Fig. 3S in Supplementary Material). However, at day 0, the emulsion stabilized with WPH at pH 8 presented the lowest volume percentage of the second peak (Fig. 3S), an thus this emulsion showed the lowest droplet size, which was significantly lower than the values obtained for emulsions stabilized with WPH at pH 2 (Table 1). In all cases, emulsions physically destabilized to some extent by flocculation or coalescence during one-week storage (Fig. 3S in Supplementary Material). The emulsion stabilized with WPH at pH 8 showed the lowest variation in droplet size during storage, increasing slightly the D[4,3] from day 0 to day 7 (Table 1). However, a more pronounced increase in droplet size was observed for the emulsion stabilized with WPH at pH 2, which showed a large increase of D[4,3] value at day 7, despite the non-significant differences registered in D[4,3] values between day 0 and day 4 (Table 1). This difference can be ascribed to the improved interfacial characteristics of WPH at pH 8 as will be discussed in detail in section 3.2.

The emulsion stabilized with BPH at pH 2 presented a significant increase in droplet size from day 0 to day 4 (Table 1). Moreover, this emulsion showed a separated oil layer at day 7, which denotes the significantly ($p < 0.05$) lower physical stability of this emulsion when compared to the emulsions stabilized with WPH (Table 1). These results correlate well with those previously reported by Padial-Domínguez (2020) for 5% fish oil-in-water emulsions stabilized with a higher concentration (2 wt% protein) of WPH at pH 8 or BPH at pH 2 (Padial-Domínguez et al., 2020).

3.2. Interfacial properties

3.2.1. Interfacial tension

Proteins are conformed by different types of amino acids with different polarity depending on their side chain. Indeed, whey and blue whiting proteins, like most proteins, present both highly hydrophobic/apolar amino acids (i.e., Trp, Ile, Phe, Leu or Val) and highly hydrophilic/polar amino acids (i.e., Lys, Arg or Glu) (Padial-Domínguez et al., 2020). The heterogeneous distribution of hydrophobic and hydrophilic amino acids within the protein backbone confers amphiphilicity to the peptides resulting from enzymatic hydrolysis. This allows amphiphilic peptides to adsorb onto the O/W interface with hydrophobic sides oriented towards the oil phase and hydrophilic sides oriented into the aqueous phase (Aguilera-Garrido, del Castillo-Santaella, Yang, et al., 2021; Del Castillo-Santaella, Cebrián, Maqueda, Gálvez-Ruiz, & Maldonado-Valderrama, 2018; García-Moreno et al., 2020). Consequently, the free energy of the system, and thus the interfacial tension, decreases upon adsorption, and this favours the formation of oil droplets during the homogenization process (McClements, 1999).

Fig. 1 and Fig. 2 show the obtained results for the time evolution of the interfacial tension when increasing bulk concentration (0.001–10 mg/mL) of WPH or BPH in the aqueous phase at pH 8 and 2. These bulk concentrations provide an estimated interfacial coverage in the pendant

Table 1
Droplet size and zeta potential of 5% fish oil-in-water emulsions stabilized with 2 wt% of whey (WPH) or blue-whiting (BPH) protein hydrolysates.

Emulsion		Zeta potential (mV)	D[4,3], μm		
			Day 0	Day 4	Day 7
WPH	pH 8	−45.8 ± 1.0 ^{u}	0.375 ± 0.008 ^{u,*}	0.551 ± 0.015 ^{u,*}	0.73 ± 0.04 ^{u,*}
	pH 2	62.5 ± 0.4 ^{v}	0.70 ± 0.06 ^{v,ns}	0.736 ± 0.006 ^{v,ns}	1.7 ± 0.4 ^{v,*}
BPH	pH 2	54.4 ± 1.8 ^{w}	0.87 ± 0.03 ^{w,*}	1.13 ± 0.18 ^{w,*}	[a]

For each column, different letter u-w indicate significant differences ($p < 0.05$) between samples.
For D4,3, for each row, * indicates significant differences ($p < 0.05$) within storage, whereas "ns" indicates not significant differences ($p > 0.05$).
[a] Emulsion showed a separated layer on the top and droplet size was not measured.

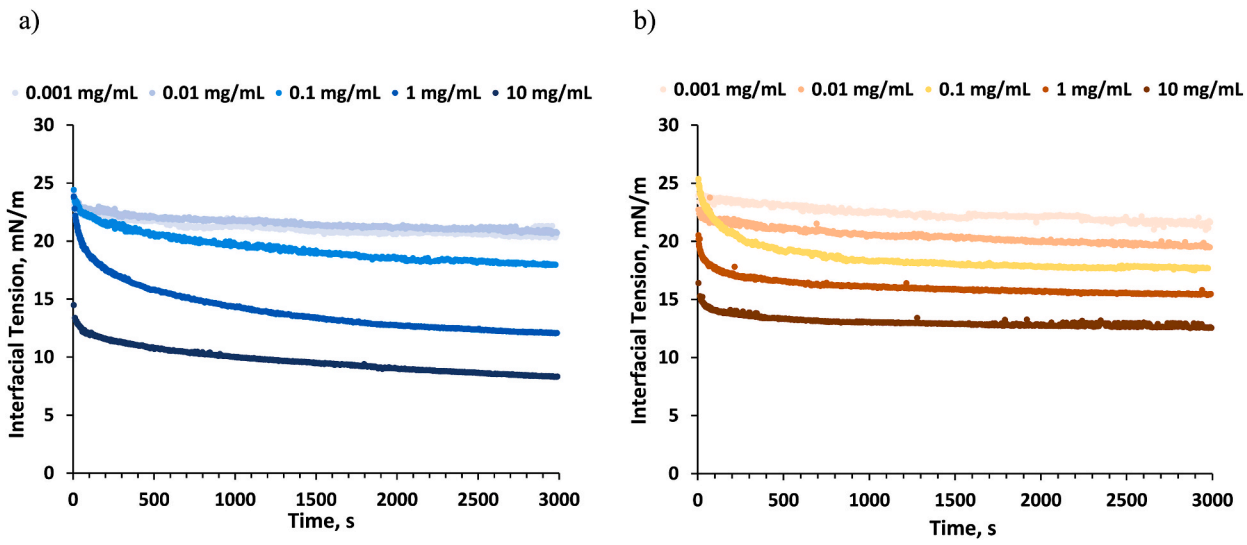

Fig. 1. Evolution of the interfacial tension at the fish oil-aqueous phase interface with increasing concentration of whey protein hydrolysate (WPH) in the aqueous phase at: a) pH 8, and b) pH 2. The bare fish oil-water interfacial tension was (24.5 ± 0.2) mN/m at T = 20 °C. The coefficient of variation within replicates for each measured time was lower than 5.6%. (For interpretation of the references to colour in this figure legend, the reader is referred to the Web version of this article.)

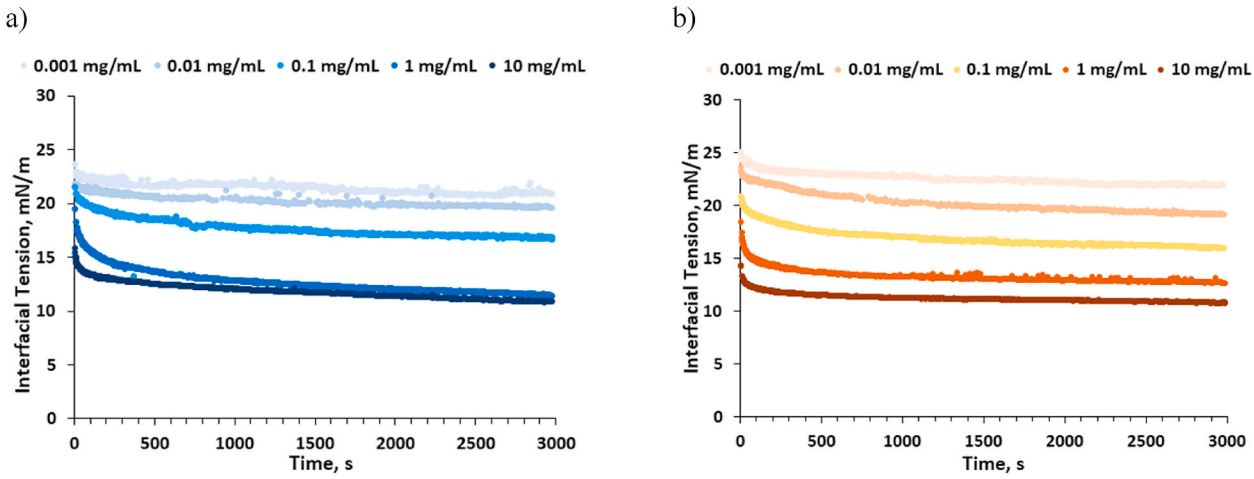

Fig. 2. Evolution of the interfacial tension at the fish oil-aqueous phase interface with increasing concentration of blue-whiting protein hydrolysate (BPH) in the aqueous phase at: a) pH 8, and b) pH 2. The bare fish oil-water interfacial tension was (24.5 ± 0.2) mN/m at T = 20 °C. The coefficient of variation within replicates for each measured time was lower than 6.8%. (For interpretation of the references to colour in this figure legend, the reader is referred to the Web version of this article.)

drop ranging between $6.4{\cdot}10^{-4}$ and 6.4 g hydrolysate/m^2. These values are comparable to the estimated interfacial coverage of emulsions of $5.32{\cdot}10^{-4}$ g hydrolysate/m^2 (WPH at pH 8 at day 0), $6.54{\cdot}10^{-4}$ g hydrolysate/m^2 (WPH at pH 2 at day 0) and $8.13{\cdot}10^{-4}$ g hydrolysate/m^2 (BPH at pH 2 at day 0). Hence, the experimental results provide a comparable interfacial layer to that formed in the emulsified systems. The highest concentrations assayed of WPH and BPH led to a rapid initial decrease of interfacial tension at both pH (Figs. 1 and 2), which was attributed to a speedily adsorption of peptides at the O/W interface during the first 200 s of measurements.

WPH causes a gradual decrease in interfacial tension when increasing time and concentration at both pHs 8 and 2 (Fig. 1). This can be explained by the continued diffusion of peptides from the bulk (aqueous phase) onto the oil-water interface with time, and by the higher peptide occupation of interfacial area, owing to the higher concentration of protein present. A similar adsorption dynamics was observed for BPH at pH 2 (Fig. 2). However, no further decrease in interfacial tension was found when increasing BPH concentration from 1 to 10 mg/mL at pH 8 (Fig. 2a), indicative of a fully covered interface. Thus, increasing concentration of BPH above 1 mg/mL at pH 8 might result in adsorption of molecules in a second layer below the interfacial layer and into the aqueous phase, interfacial aggregation or gelation processes which do not affect the interfacial tension (Maldonado--Valderrama et al., 2005). Similar results were obtained with human serum albumin (HSA) and bovine serum albumin (BSA) proteins when the oil-water interface was saturated (Aguilera-Garrido, del Castillo-Santaella, Yang, et al., 2021; Del Castillo-Santaella et al., 2018; Maldonado-Valderrama et al., 2005).

Interestingly, pH significantly influenced the degree of adsorption of WPH at the O/W interface as reflected in the reduction of the interfacial tension. Fig. 3a shows that for the highest concentrations assayed of WPH (1 and 10 mg/mL), the final interfacial tension obtained was significantly ($p < 0.05$) lower at pH 8 when compared to pH 2 (see also Table 1S in Supplementary Material for the statistical analysis). The influence of pH on the rate and degree of interfacial adsorption is also related with the conformational state of peptides (molecular size,

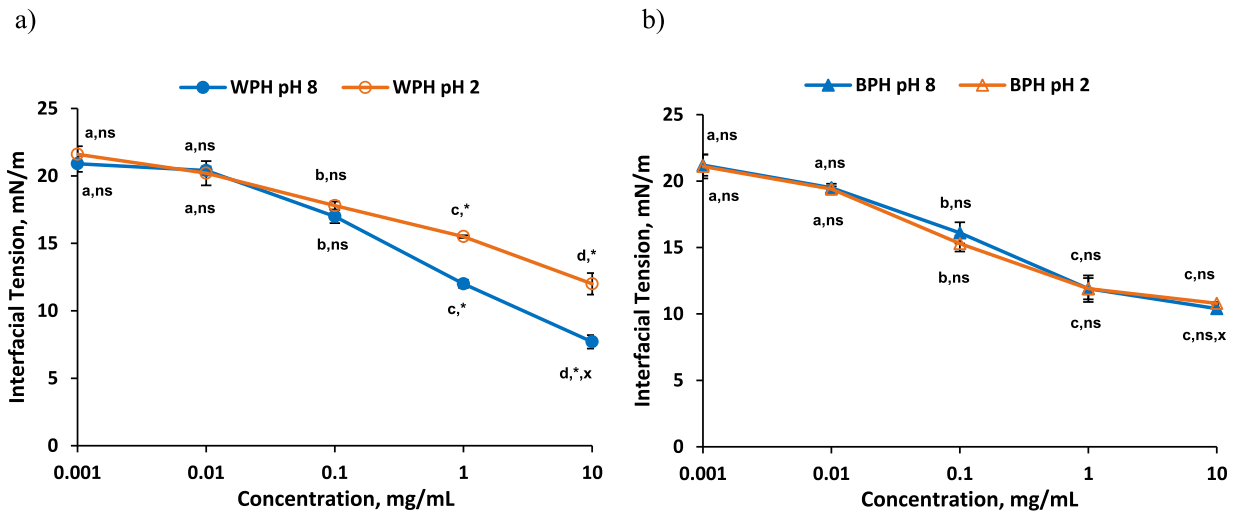

Fig. 3. Final values (at 3000 s) of interfacial tension at the fish oil/aqueous phase interface with increasing concentrations of a) whey protein (WPH) and b) blue-whiting (BPH) protein hydrolysates in the aqueous phase at pH 8 and 2. The bare fish oil-water interfacial tension was (24.5 ± 0.2) mN/m at T = 20 °C. Statistical treatment of the data is shown in Table 1 S. Different letters a–d indicate significant differences ($p < 0.05$) with concentration at pH 8 or 2. * indicates significant differences ($p < 0.05$) between pH for the same type of hydrolysate, whereas "ns" indicates not significant differences ($p > 0.05$). x indicates significant differences ($p < 0.05$) between types of hydrolysates for the same pH and concentration. (For interpretation of the references to colour in this figure legend, the reader is referred to the Web version of this article.)

structure, hydrodynamic radius) and the chemical nature of the peptides surface (charge and hydrophobicity) (Felix et al., 2019). Particularly, the charge of the amino acids constituting the peptides is a key factor affecting interfacial adsorption, since it highly determines the peptides solubility (Damodaran, 2017). For instance, acidic proteins/peptides, those with higher percentage of Asp + Glu than Lys + Arg + His, present maximum solubility at alkaline pH. On the other hand, alkaline proteins/peptides, those with lower percentage of Asp + Glu than Lys + Arg + His, show maximum solubility at acid pH values (Damodaran, 2017). WPH presents a higher molar percentage of Asp + Glu balance (26.4%) than Lys + Arg + His (13.6%) (Padial-Domínguez et al., 2020), indicating an acidic protein behaviour and in consequence a higher solubility at alkaline pH values when compared to acidic pH. An increase in the solubility of amphiphilic peptides favours their diffusion to the O/W interface, which is of particular importance in the experiments carried out at the drop tensiometer, where mass transfer of peptides from the aqueous phase to the oil-water interface is diffusion-controlled (Schröder et al., 2017). Therefore, a faster diffusion of peptides onto the interface together with the appropriate unfolding, the latter being determined by the presence of hydrophobic regions, may explain these lower interfacial tension values obtained for the highest concentrations of WPH at pH 8 when compared to pH 2 (Fig. 3a). On the contrary, BPH did not show significant ($p > 0.05$) differences in the final interfacial tension obtained at pH 8 and 2 in the range of concentrations assayed (Fig. 3b), which indicates a low influence of pH on adsorption of peptides present in BPH. This may be attributed to the only slightly basic character of BPH, with an amino acids balance Asp + Glu (21.8%) slightly lower to Lys + Arg + His (25.4%) (Padial-Domínguez et al., 2020), which may denote similar solubility of BPH at alkaline and acidic pHs.

Fig. 3 also shows the lower values of interfacial tension at the highest hydrolysate concentration (10 mg/mL) for WPH at pH 8 compared with BPH at any pH value in spite of the higher protein concentration present in BPH (76.8%) compared with WPH (32.7%). This finding can be attributed to the different size of the peptides present in each hydrolysate. WPH presents more than 50% of peptides of large (>10 kDa) and medium (3–10 kDa) size, while BPH presents mainly (~80%) low-size peptides (<3 kDa) (Padial-Domínguez et al., 2020). A minimum length of peptide (>13–18 amino acids) is normally required to show high amphiphilicity and properly re-arrange (i.e., as β-strand or α-helix) at the O/W interface stabilizing oil-in-water emulsions (García-Moreno et al., 2021). In addition, WPH has higher content of non-polar amino acids such as Ala, Gly, Leu, Ile, Met, Phe, Pro, Val (46.9%) when compared to BPH (40.1%) (Padial-Domínguez et al., 2020). Higher content of non-polar amino acids implies increasing surface hydrophobicity (Benjamin, Silcock, Beauchamp, Buettner, & Everett, 2014), which favours the anchoring of peptides at the O/W interface, explaining the lower interfacial tension attained by WPH (McClements, 1999). The differences in peptide size distribution of the hydrolysates are attributed to the solubility of the substrates (i.e., whey or blue whiting proteins) used in the enzymatic hydrolysis. Blue whiting protein is not soluble, and thus is in suspension during enzymatic hydrolysis, which means that the fragments of proteins released and solubilized by the action of trypsin can be more easily further broken down in solution by the soluble enzyme. This reveals why BPH, with DH 4% but only containing soluble peptides, presents shorter peptides when compared to WPH at DH 10% since whey protein is soluble and thus subtilisin can equally act on either soluble intact protein or released peptides.

The lower interfacial tension values observed for WPH at pH 8 when compared to pH 2 during the first 500 s, indicates the rapid interfacial coverage of this interface, hence facilitating the disruption of oil droplets, resulting in the formation of smaller droplets during homogenization for a certain energy input as can be observed in Table 1 (McClements, 1999). On the other hand, the lower adsorption of peptides present in BPH onto the O/W interface resulted in a significant less reduction of the interfacial tension (Fig. 3 and Table 1S), possibly responsible for the larger droplet sizes in the emulsion (Table 1). A reduced interfacial coverage would also promote emulsion destabilization for example by creaming, hence explaining the separated oil layer on the top of the emulsion stabilized with BPH at pH 2 observed at day 7 since the velocity of creaming is directly proportional to the square of the droplet diameter.

It is worth mentioning that similar final interfacial tension values (after 3 h) (12–16 mN/m) were previously reported for WPH with different DH for MCT (medium chain triglycerides) oil/water interfaces at a protein concentration of 0.1 mg/mL (Schröder et al., 2017). The slightly higher values of final interfacial tension observed in this study are explained by the differences in protein content and DH between WPHs as well as by the lower equilibrium interfacial tension of pure oil MCT/water interface (18–20 mN/m) compared to pure fish oil/water

interface (23–24 mN/m). Morales-Medina et al. (2016) reported final interfacial tension values (MCT oil/water, after 30 min) ranging from 5.3 to 13 mN/m for sardine and horse mackerel hydrolysates at 2 or 0.1 wt% obtained by subtilisin or trypsin at pH 2. This is in the line of the interfacial tension obtained in this study for BPH (10.8 ± 0.1 mN/m) at 10 mg/mL (1 wt%) at pH 2 for fish oil/water interface (Fig. 3b).

3.2.2. Dilatational rheology

Dilatational rheology of interfaces, which is based in the application of volume variations keeping a constant shape, provides information about interfacial structure, intermolecular connections, interfacial conformation and viscoelasticity of the interfacial layer (Del Castillo-Santaella et al., 2018; Maldonado-Valderrama & Rodríguez, 2010; Maldonado-Valderrama et al., 2015). The complex dilatational modulus of the interfacial layer, E, determines the capacity of response of the interfacial film to a perturbation of its equilibrium state, providing information about the viscoelastic behaviour of the interface. Thus, E is formed by: i) an elastic component, E′, which matches with the interfacial elasticity (ε_d) and ii) a viscous part, E″, equal to the product of frequency and interfacial viscosity (η_d) according to Eq. (2). In this way, ε_d represents the resistance of the interfacial layer to adapt to area changes and the speed at which the interfacial tension gradients disappear once the deformation is cease, while η_d represents the existence of relaxation processes near or at the interface (Maldonado-Valderrama et al., 2015; Maldonado-Valderrama & Rodríguez, 2010).

According to the interfacial rheology, the behaviour of the interfacial layer was mostly elastic, with E' > E″, which translates in interfacial elasticity values very close to E values (Tables 2S and 3S in Supplementary Material).

Isothermal graphical representations of interfacial dilatational rheology were carried out for each hydrolysate at pH 8 and 2 for a frequency of 0.1 Hz (Fig. 4), providing fundamental information about the evolution of the complex dilatational modulus of the interfacial layer (E) when increasing concentration of hydrolysates. 0.1 Hz was the selected frequency as it is a medium/high frequency value, widely reported in literature, without presenting the large variability of the measured values caused by the fast perturbation at 1 Hz and avoiding the larger viscous component (or loss modulus) data at 0.01 Hz.

Interestingly, the E of the adsorbed layer of WPH as a function of pH showed a complex dependence with the interfacial coverage. While significantly ($p < 0.05$) higher E values were obtained for WPH at pH 8 when compared to pH 2 at intermediate interfacial coverage (0.1 and 1 mg/mL), lower E values were obtained at the lowest (0.001, 0.01 mg/mL) and highest interfacial coverages (10 mg/mL) (Fig. 4a). These findings reveal the formation of an interfacial stretchable layer of WPH-containing peptides with a superior consistency and strength at pH 8 once a critical interfacial coverage is reached. This interfacial coverage matches the values at the emulsion droplet and the higher E obtained at pH 8 would explain the lower droplet size variations experimented during storage of the emulsion stabilized with WPH at pH 8 (Table 1), and in consequence its greater resistance against potential destabilization mechanisms (Maldonado-Valderrama et al., 2008). It should be noted that the interfacial coverage is comparable to that of emulsions for concentrations in the pendant drop up to 0.1 mg/mL as explained above. The influence of pH on E values could be attributed to the charges of the amino acids present in the peptides, where the acidic character of WPH peptides would propitiate a higher solubility, adsorption and increased unfolding of peptides at the O/W interface at alkaline pH when compared to acidic pH. The values of E obtained in Fig. 4 are similar to those obtained with Albumins adsorbed at oil-water interface at a similar oscillation frequency, which also form stable emulsions (result not published yet). At the highest bulk concentration, the E obtained at pH 8 provides a similar value to the previous concentration while it continues to increase for WPH at pH 2 (Fig. 4a). This could be explained by to the lower interfacial tension of WPH at pH 8 (Fig. 3a) which implies a higher interfacial coverage, which in turn prevents further unfolding of peptides due to the formation of a compact interfacial layer (Maldonado-Valderrama et al., 2005).

The behaviour of the E of BPH as a function of pH is different to that of WPH. Fig. 4b shows now significantly ($p < 0.05$) lower values of E for BPH at pH 8 when compared to pH 2 for 0.1 Hz above a critical interfacial coverage (c > 0.1 mg/mL). This indicates the formation of a weaker interfacial peptide layer at pH 8 than at pH 2 for BPH. This might be related to the slight basic character of BPH peptides, resulting in slightly lower solubility of fish proteins at alkaline pH (Petursson et al., 2004). Although the potential difference in solubility and surface charge of peptides due to pH did not significantly influenced the reduction of interfacial tension in BPH (Fig. 3), it did affect the unfolding and interaction of peptides at the O/W interface. Despite the higher E values obtained for BPH at pH 2 at 0.1, 1 and 10 mg/mL when compared to

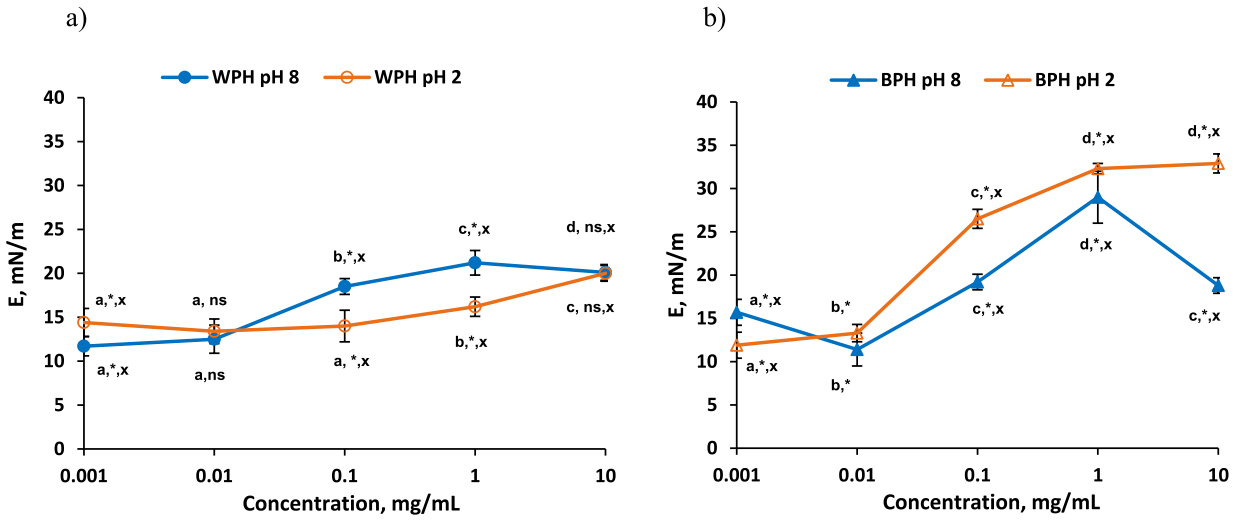

Fig. 4. Complex surface dilatational modulus for fish oil−water interfaces stabilized by a) whey protein hydrolysate (WPH), or b) blue-whiting protein hydrolysate (BPH) as a function of pH and concentration. Frequency: 0.1 Hz. Amplitude of deformation: 5%. Temperature 20 °C. Different letters a-d indicate significant differences ($p < 0.05$) with concentration at pH 8 or 2. * indicates significant differences ($p < 0.05$) between pH for the same type of hydrolysate, whereas "ns" indicates not significant differences ($p > 0.05$). x indicates significant differences ($p < 0.05$) between types of hydrolysates for the same pH and concentration. (For interpretation of the references to colour in this figure legend, the reader is referred to the Web version of this article.)

WPH-stabilized interfaces (Fig. 4), both creaming and higher increase in droplet size (Table 1) indicate a lower physical stability for the emulsion stabilized with BPH at pH 2. This could mean that although BPH at pH 2 showed a higher complex dilatational modulus, indicative of stronger interpeptide interactions at the interface as compared to WPH (Fig. 4), the lower adsorption degree of BPH when compared to WPH resulted in an insufficient peptide coating of the oil droplet allowing flocculation and coalescence of oil droplets in the emulsion (Table 1). In a real situation, both shear and dilatational deformations are present at the interface. Hence, in order to fully account for the behavior encountered in emulsions it would be useful to characterize the shear rheology both of emulsions and of the interfacial layer. This would definitely provide additional information on intermolecular interactions at the interface (Rühs et al., 2013).

Fig. 4 (see also Table 2S in Supplementary Material) shows a general increase in E values at frequencies of 1, 0.1 Hz and 0.01 Hz when increasing the concentration of hydrolysates. This finding is explained by a higher adsorption of peptides at the interface when increasing concentration, which increases peptides interactions at the interface as well as thickness of the interfacial film. The latter results in a denser, more compact and more elastic interface (Maldonado-Valderrama, 2006). Most of the exceptions to this trend between E and concentration are attributed to a complete occupation of the interface in terms of free energy, phenomenon clearly observed in BPH between 1 and 10 mg/mL where the final values of interfacial tension levelled off (Fig. 3). Moreover, Fig. 4 showed a maximum in E values for a concentration of BPH of 1 mg/mL at pH 8. After reaching a maximum the elasticity of the interfacial layer is reduced indicating alterations in the cohesive structure of the interface (Maldonado-Valderrama, Muros-Cobos, Holgado--Terriza, & Cabrerizo-Vílchez, 2014; Pérez-Mosqueda, Maldonado-Valderrama, Ramírez, Cabrerizo-Vílchez, & Muñoz, 2013; Torcello-Gómez et al., 2013). These alterations in E could be originated by the formation of peptide multilayers at the interface, formation of interfacial aggregates or molecular reorientation (Pérez-Mosqueda et al., 2013). These relaxation phenomena promote changes in elasticity when applying a deformation to the interface (Del Castillo-Santaella et al., 2018; Maldonado-Valderrama & Rodríguez, 2010). Interestingly, these relaxation phenomena are only detected for BPH at pH 8 as the E decreases significantly and might explain the break of the emulsion stabilized with BPH at pH 8.

In order to deepen into the relaxation phenomena occurring at the interfacial layer, Fig. 5 shows the influence of the frequency on the elasticity of the interfacial layer at a concentration of 0.1 mg/mL, representative of enough interfacial coverage to provide stable emulsions (Del Castillo-Santaella et al., 2018; Schröder et al., 2017) and with a comparable but above interfacial coverage to that of emulsions on both WPH and BPH. At this concentration, the dilatational elasticity of WPH (Fig. 5a) and BPH (Fig. 5b) significantly ($p < 0.05$) increased when increasing frequency at pH 8 and pH 2. This was expected since at higher frequency values, the layer has less time to adapt to the deformation, which results in higher ε_d values. On the other hand, at low frequencies, the interfacial layer has more time to adapt to the deformation, resulting in lower ε_d values (Maldonado-Valderrama, 2006; Maldonado--Valderrama et al., 2014). In addition, and in agreement with E values, WPH showed a higher interfacial elasticity at pH 8 when compared to pH 2 at 0.01, 0.1 and 1 Hz, whereas the opposite trend was observed for BPH at 0.01 and 0.1 Hz. These findings further denote the influence of pH on the re-arranging of WPH and BPH peptides at the fish oil-water interface and it deserves further research to elucidate secondary structure of peptides at the O/W interface.

Schröder et al. (2017) reported elasticity values (12–25 mN/m) for WPHs (obtained at 0.1 mg/mL, frequency of 0.05 Hz, 5% amplitude, oil MCT/water) comparable to the results obtained in this study for WPH at 0.1 mg/mL and 0.1–0.01 Hz: 11.9 ± 1.3–18.5 ± 0.9 mN/m (Fig. 5a and Table 3S). In agreement with our results, Schröder et al. compared WPI and WPH hydrolysates, which showed that stronger oil-water interfacial layers with minor interfacial tension values and high dilatational moduli were correlated with higher protein surface coverage and emulsions with improved stability (Schröder et al., 2017). Del Castillo-Santaella et al. (2014) reported elasticity values for β-lactoglobulin, one of the principal proteins present in WPH, at a concentration of 0.1 mg/mL for an olive oil/water interface at frequencies of 1 Hz (32 ± 3 mN/m), 0.1 Hz (26 ± 3 mN/m) and 0.01 Hz (22 ± 3 mN/m), which are higher values than those found in this work (Table 3S). This is explained by the stronger interfacial network developed by β-lactoglobulin, a globular protein retaining some secondary structure at the interfacial layer, which leads to stiffer interfaces owing also to a larger degree of unfolding and interaction at the O/W interface (McClements, 1999). To the best of our knowledge, there are not previous studies on dilatational rheology for oil/water interfaces stabilized with fish protein hydrolysates.

An opposite trend was observed for interfacial dilatational viscosity

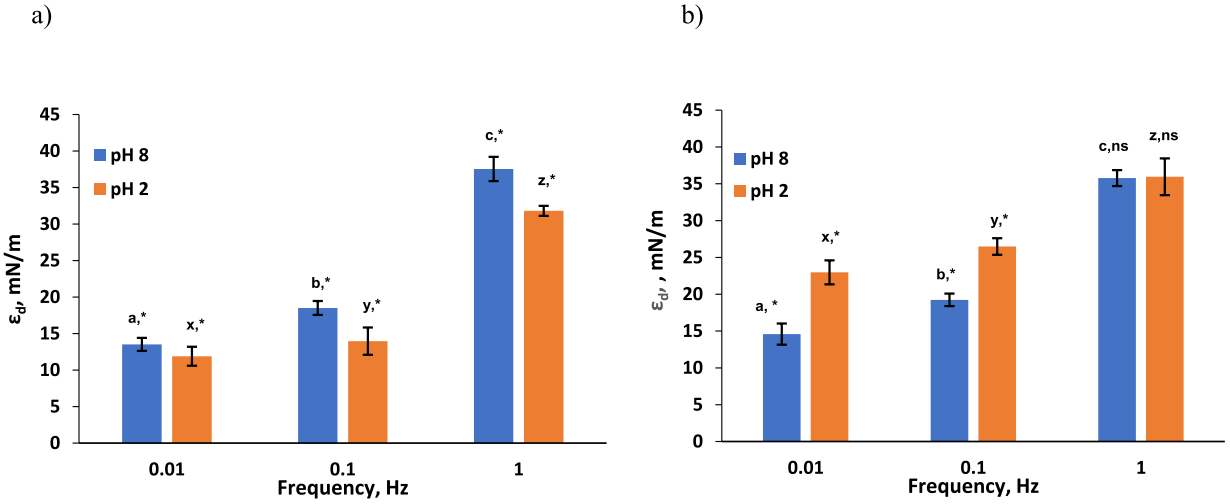

Fig. 5. Interfacial elasticity (ε_d) for fish oil−water interfaces stabilized by a) whey protein hydrolysate (WPH), or b) blue-whiting protein hydrolysate (BPH) (0.1 mg/mL, 20 °C) as a function of pH and frequency (0.01–1 Hz). Amplitude of deformation: 5%. Temperature 20 °C. Different letters a-c or x-z indicate significant differences ($p < 0.05$) with frequency for pH 8 and 2, respectively. For each frequency, * indicates significant differences ($p < 0.05$) between pH 8 and 2, whereas "ns" indicates not significant differences ($p > 0.05$). (For interpretation of the references to colour in this figure legend, the reader is referred to the Web version of this article.)

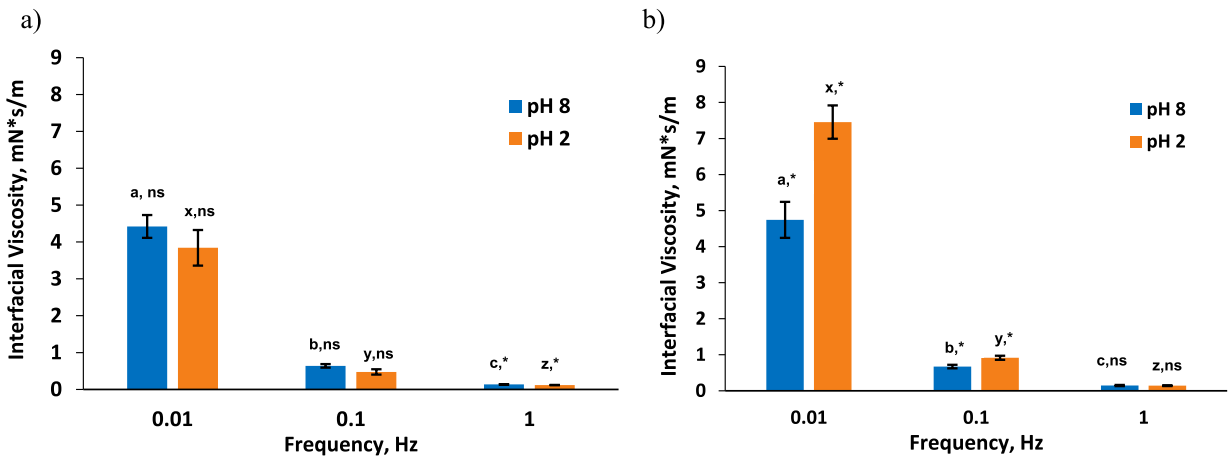

Fig. 6. Interfacial dilatational viscosity for fish oil−water interfaces stabilized by a) whey protein hydrolysate (WPH), or b) blue-whiting protein hydrolysate (BPH) (0.1 mg/mL, 20 °C) as a function of pH and frequency (0.01–1 Hz). Amplitude of deformation: 5%. Temperature 20 °C. Different letters a-c or x-z indicate significant differences ($p < 0.05$) with frequency for pH 8 and 2, respectively. For each frequency, * indicates significant differences ($p < 0.05$) between pH, whereas "ns" indicates not significant differences ($p > 0.05$). (For interpretation of the references to colour in this figure legend, the reader is referred to the Web version of this article.)

when varying frequency, decreasing apparent interfacial dilatational viscosity when increasing frequency (Fig. 6). As anticipated above, this is ascribed to the occurrence of relaxation phenomena at the interface at lower frequencies (Maldonado-Valderrama et al., 2005, 2014). Hence, only the values at 0.01 and 0.1 Hz will be comparatively analysed. It is remarkable that not significant differences were observed in interfacial dilatational viscosity for WPH at different pH (at 0.01 and 0.1 Hz) (Fig. 6a). However, BPH showed significantly higher interfacial dilatational viscosity at pH 2 when compared to pH 8 (at 0.01 and 0.1 Hz) (Fig. 6b). This could be also originated by differences in the molecular conformation of BPH at pH 2 compared to pH 8, which result in improved emulsion stabilisation.

The values obtained for the interfacial dilatational viscosity measured at 0.01, 0.1 and 1 Hz for WPH and BPH at different concentrations are displayed in Table 4S. A maximum is shown for 1 mg/mL BPH at pH 8 (7.2 ± 0.8 mN/m s) at 0.01 Hz, which coincides with the maximum for the elasticity for the same concentration of BPH at pH 8, 0.01 Hz discussed above. The presence of a maximum is indicative of alterations in the distribution of molecules in the monolayer, due to the formation of multilayers, aggregation or molecular reorientations at the interfacial layer (Pérez-Mosqueda et al., 2013). These conformational changes can prevent the formation of a homogeneous interfacial layer, resistant to deformations, and originate the possible rupture of emulsion as it was experimented in the case of BPH at pH 8. The rest of systems evaluated do not show a maximum, in agreement with the formation of more stable emulsions. The correlation between interfacial elasticity/-viscosity and emulsion stabilisation is not straightforward, but provides some clues on the interfacial origins of emulsion behaviour at the molecular level. Interfacial conformation and interactions are key factors determining the response of interfacial layers to deformation which can be crucial in the understanding of emulsion behaviour.

4. Conclusions

The interfacial properties (interfacial adsorption and dilatational rheology) of WPH and BPH allowed to explain differences in the physical stability of fish oil-in-water emulsions stabilized with these hydrolysates at pH 8 or 2. WPH presented higher interfacial activity (i.e., lower interfacial tension values) than BPH at pH 8 and 2 despite its lower protein content, which was attributed to the superior content of high-molecular weight peptides in WPH than can further unfold at the O/W interface when compared to shorter peptides present in BPH. Interestingly, the charge of the peptides was a key factor in the interfacial behaviour of the hydrolysates, affecting directly to their solubility and unfolding at different pH based in the acidic/alkaline balance of the peptides in the hydrolysate. Thus, the superior acidity of the peptides present in WPH might be responsible for its higher interfacial activity and stronger interfacial film at pH 8. This correlated with the higher physical stability of the emulsion stabilized with WPH at pH 8 when compared to pH 2. On the contrary, BPH, containing peptides with only a slightly superior alkalinity, did not show significant different on interfacial tension at pH 2 and 8. Nevertheless, pH turned out to significantly affect the viscoelasticity and consistency of the peptide interfacial film formed by peptides in BPH. Negative surface charge of BPH peptides at alkaline pH resulted in more unfavourable unfolding leading to lower E values, and thus lower interfacial elasticity and dilatational viscosity for BPH-stabilized interfaces at pH 8 when compared to pH 2. It might explain the immediate break of the BPH-stabilized emulsion at pH 8 after homogenization, which was not observed for the BPH-stabilized emulsion at pH 2. Thus, this work provides new understanding on the interfacial properties of blue whiting protein hydrolysate, which might contribute to pave the way for the use of fish protein hydrolysates as emulsifiers.

Author contributions

José María Ruiz-Álvarez: Formal analysis, Writing – original draft. Teresa del Castillo-Santaella: Conceptualization, Methodology, Supervision, Writing - review and editing. Julia Maldonado-Valderrama: Conceptualization, Methodology, Writing - review and editing. Antonio Guadix: Writing - review and editing. Emilia Guadix: Writing - review and editing, Funding acquisition. Pedro J. García-Moreno: Conceptualization, Methodology, Supervision, Writing - review and editing.

Declaration of competing interest

The authors declare that they have no known competing financial interests or personal relationships that could have appeared to influence the work reported in this paper.

Acknowledgements

This work was funded by the project CTQ2017-87076-R from the Spanish Ministry of Science and Innovation. Julia Maldonado-Valderrama and Teresa del Castillo-Santaella acknowledge financial

support from project RTI2018-101309-B-C21. The authors are also very grateful to F. Javier Espejo-Carpio and Marta Padial-Domínguez for providing the whey and blue whiting protein hydrolysates. Funding for open access charge: Universidad de Granada / CBUA.

Appendix A. Supplementary data

Supplementary data to this article can be found online at https://doi.org/10.1016/j.foodhyd.2021.107075.

References

Aguilera-Garrido, A., del Castillo-Santaella, T., Galisteo-González, F., José Gálvez-Ruiz, M., & Maldonado-Valderrama, J. (2020). Investigating the role of hyaluronic acid in improving curcumin bioaccessibility from nanoemulsions. *Food Chemistry, 351*. https://doi.org/10.1016/j.foodchem.2021.129301, 2021.

Aguilera-Garrido, A., del Castillo-Santaella, T., Yang, Y., Galisteo-González, F., Gálvez-Ruiz, M. J., Molina-Bolívar, J. A., et al. (2021). Applications of serum albumins in delivery systems: Differences in interfacial behaviour and interacting abilities with polysaccharides. *Advances in Colloid and Interface Science, 290*, 102365. https://doi.org/10.1016/j.cis.2021.102365

Arab-Tehrany, E., Jacquot, M., Gaiani, C., Imran, M., Desobry, S., & Linder, M. (2012). Beneficial effects and oxidative stability of omega-3 long-chain polyunsaturated fatty acids. *Trends in Food Science & Technology, 25*(1), 24–33. https://doi.org/10.1016/j.tifs.2011.12.002

Arnardottir, H., Pawelzik, S. C., Öhlund Wistbacka, U., Artiach, G., Hofmann, R., Reinholdsson, I., et al. (2021). Stimulating the resolution of inflammation through omega-3 polyunsaturated fatty acids in COVID-19: Rationale for the COVID-omega-F trial. *Frontiers in Physiology, 11*(January), 1–7. https://doi.org/10.3389/fphys.2020.624657

Belury, M. A. (2002). Inhibition of carcinogenesis by conjugated linoleic acid: Potential mechanisms of action. *Journal of Nutrition, 132*(10), 2995–2998. https://doi.org/10.1093/jn/131.10.2995

Benjamin, O., Silcock, P., Beauchamp, J., Buettner, A., & Everett, D. W. (2014). Emulsifying properties of legume proteins compared to β-lactoglobulin and tween 20 and the volatile release from oil-in-water emulsions. *Journal of Food Science, 79*(10), E2014–E2022. https://doi.org/10.1111/1750-3841.12593

Berton-Carabin, C. C., Ropers, M. H., & Genot, C. (2014). Lipid oxidation in oil-in-water emulsions: Involvement of the interfacial layer. *Comprehensive Reviews in Food Science and Food Safety, 13*(5), 945–977. https://doi.org/10.1111/1541-4337.12097

Bimbo, A. P. (2013). Sources of omega-3 fatty acids. In *Food enrichment with omega-3 fatty acids*. https://doi.org/10.1533/9780857098863.1.27

Brenna, J. T., Salem, N., Sinclair, A. J., & Cunnane, S. C. (2009). α-Linolenic acid supplementation and conversion to n-3 long-chain polyunsaturated fatty acids in humans. *Prostaglandins Leukotrienes and Essential Fatty Acids, 80*(2–3), 85–91. https://doi.org/10.1016/j.plefa.2009.01.004

Cabrerizo-Vílchez, M. A., Wege, H. A., Holgado-Terriza, J. A., & Neumann, A. W. (1999). Axisymmetric drop shape analysis as penetration Langmuir balance. *Review of Scientific Instruments, 70*(5), 2438–2444. https://doi.org/10.1063/1.1149773

Carrera Sánchez, C., & Rodríguez Patino, J. M. (2021). Contribution of the engineering of tailored interfaces to the formulation of novel food colloids. *Food Hydrocolloids, 119*, 106838. https://doi.org/10.1016/j.foodhyd.2021.106838

Damodaran, S. (2017). Amino acids, peptides, and proteins. In *Fennema's food chemistry* (pp. 219–329). CRC Press LLC.

Del Castillo-Santaella, T., Cebrián, R., Maqueda, M., Gálvez-Ruiz, M. J., & Maldonado-Valderrama, J. (2018). Assessing in vitro digestibility of food biopreservative AS-48. *Food Chemistry, 246*, 249–257. https://doi.org/10.1016/j.foodchem.2017.10.149

Del Castillo-Santaella, T., Sanmartín, E., Cabrerizo-Vílchez, M. A., Arboleya, J. C., & Maldonado-Valderrama, J. (2014). Improved digestibility of β-lactoglobulin by pulsed light processing: A dilatational and shear study. *Soft Matter, 10*(48), 9702–9714. https://doi.org/10.1039/c4sm01667j

Elagizi, A., Lavie, C. J., Marshall, K., DiNicolantonio, J. J., O'Keefe, J. H., & Milani, R. V. (2018). Omega-3 polyunsaturated fatty acids and cardiovascular health: A comprehensive review. *Progress in Cardiovascular Diseases, 61*(1), 76–85. https://doi.org/10.1016/j.pcad.2018.03.006

Felix, M., Romero, A., Carrera-sanchez, C., & Guerrero, A. (2019). Food Hydrocolloids Assessment of interfacial viscoelastic properties of Faba bean (Vicia faba) protein-adsorbed O/W layers as a function of pH. *Food Hydrocolloids, 90*(August 2018), 353–359. https://doi.org/10.1016/j.foodhyd.2018.12.036

García-Moreno, P. J., Gregersen, S., Nedamani, E. R., Olsen, T. H., Marcatili, P., Overgaard, M. T., et al. (2020). Identification of emulsifier potato peptides by bioinformatics: Application to omega-3 delivery emulsions and release from potato industry side streams. *Scientific Reports, 10*(1), 1–22. https://doi.org/10.1038/s41598-019-57229-6

García-Moreno, P. J., Guadix, A., Guadix, E. M., & Jacobsen, C. (2016). Physical and oxidative stability of fish oil-in-water emulsions stabilized with fish protein hydrolysates. *Food Chemistry, 203*, 124–135. https://doi.org/10.1016/j.foodchem.2016.02.073

García-Moreno, P. J., Horn, A. F., & Jacobsen, C. (2014). Influence of casein-phospholipid combinations as emulsifier on the physical and oxidative stability of fish oil-in-water emulsions. *Journal of Agricultural and Food Chemistry, 62*(5), 1142–1152. https://doi.org/10.1021/jf405073x

García-Moreno, P. J., Yang, J., Gregersen, S., Jones, N. C., Berton-Carabin, C. C., Sagis, L. M. C., et al. (2021). The structure, viscoelasticity and charge of potato peptides adsorbed at the oil-water interface determine the physicochemical stability of fish oil-in-water emulsions. *Food Hydrocolloids, 115*. https://doi.org/10.1016/j.foodhyd.2021.106605, 2020.

Gbogouri, G. A., Linder, M., Fanni, J., & Parmenter, M. (2004). C : Food chemistry and toxicology influence of hydrolysis degree. *Journal of Food Science, 69g*(8), 615–622. https://doi.org/10.1111/j.1365-2621.2004.tb09909.x

Guzey, D., Kim, H. J., & McClements, D. J. (2004). Factors influencing the production of o/w emulsions stabilized by β-lactoglobulin-pectin membranes. *Food Hydrocolloids, 18*(6), 967–975. https://doi.org/10.1016/j.foodhyd.2004.04.001

Maldonado-Valderrama, J. (2006). *Caracterización interfacial de proteínas y tensioactivos aplicación a dispersiones alimentarias*. Editorial de la Universidad de Granada.

Maldonado-Valderrama, J., Fainerman, V. B., Gálvez-Ruiz, M. J., Martín-Rodriguez, A., Cabrerizo-Vílchez, M. A., & Miller, R. (2005). Dilatational rheology of β-casein adsorbed layers at liquid-fluid interfaces. *Journal of Physical Chemistry B, 109*(37), 17608–17616. https://doi.org/10.1021/jp050927r

Maldonado-Valderrama, J., Martín-Rodriguez, A., Gálvez-Ruiz, M. J., Miller, R., Langevin, D., & Cabrerizo-Vílchez, M. A. (2008). Foams and emulsions of β-casein examined by interfacial rheology. *Colloids and Surfaces A: Physicochemical and Engineering Aspects, 323*(1–3), 116–122. https://doi.org/10.1016/j.colsurfa.2007.11.003

Maldonado-Valderrama, J., Muros-Cobos, J. L., Holgado-Terriza, J. A., & Cabrerizo-Vílchez, M. A. (2014). Bile salts at the air-water interface: Adsorption and desorption. *Colloids and Surfaces B: Biointerfaces, 120*, 176–183. https://doi.org/10.1016/j.colsurfb.2014.05.014

Maldonado-Valderrama, J., & Rodríguez, J. M. (2010). Interfacial rheology of protein-surfactant mixtures. *Current Opinion in Colloid & Interface Science, 15*(4), 271–282. https://doi.org/10.1016/j.cocis.2009.12.004

Maldonado-Valderrama, J., Terriza, J. A. H., Torcello-Gómez, A., & Cabrerizo-Vílchez, M. A. (2013). In vitro digestion of interfacial protein structures. *Soft Matter, 9*(4), 1043–1053. https://doi.org/10.1039/c2sm26843d

Maldonado-Valderrama, J., Torcello-Gómez, A., Del Castillo-Santaella, T., Holgado-Terriza, J. A., & Cabrerizo-Vílchez, M. A. (2015). Subphase exchange experiments with the pendant drop technique. *Advances in Colloid and Interface Science, 222*, 488–501. https://doi.org/10.1016/j.cis.2014.08.002

McClements, D. J. (1999). *Food emulsions. Principles, practice, and techniques*. CRC Press LLC.

Miguel, G. A., Jacobsen, C., Prieto, C., Kempen, P. J., Lagaron, J. M., Chronakis, I. S., et al. (2019). Oxidative stability and physical properties of mayonnaise fortified with zein electrosprayed capsules loaded with fish oil. *Journal of Food Engineering, 263* (May), 348–358. https://doi.org/10.1016/j.jfoodeng.2019.07.019

Morales-Medina, R., Tamm, F., Guadix, A. M., Guadix, E. M., & Drusch, S. (2016). Functional and antioxidant properties of hydrolysates of sardine (S. pilchardus) and horse mackerel (T. mediterraneus) for the microencapsulation of fish oil by spray-drying. *Food Chemistry, 194*, 1208–1216. https://doi.org/10.1016/j.foodchem.2015.08.122

Nielsen, N. S., & Jacobsen, C. (2009). Methods for reducing lipid oxidation in fish-oil-enriched energy bars. *International Journal of Food Science and Technology, 44*(8), 1536–1546. https://doi.org/10.1111/j.1365-2621.2008.01786.x

Padial-Domínguez, M., Espejo-Carpio, F. J., García-Moreno, P. J., Jacobsen, C., & Guadix, E. M. (2020). Protein derived emulsifiers with antioxidant activity for stabilization of omega-3 emulsions. *Food Chemistry, 329*(May), 127148. https://doi.org/10.1016/j.foodchem.2020.127148

Pérez-Mosqueda, L. M., Maldonado-Valderrama, J., Ramírez, P., Cabrerizo-Vílchez, M. A., & Muñoz, J. (2013). Interfacial characterization of Pluronic PE9400 at biocompatible (air-water and limonene-water) interfaces. *Colloids and Surfaces B: Biointerfaces, 111*, 171–178. https://doi.org/10.1016/j.colsurfb.2013.05.029

Petursson, S., Decker, E. A., & McClements, D. J. (2004). Stabilization of oil-in-water emulsions by cod protein extracts. *Journal of Agricultural and Food Chemistry, 52*(12), 3996–4001. https://doi.org/10.1021/jf035251g

Rahali, V., Chobert, J. M., Haertlé, T., & Guéguen, J. (2000). Emulsification of chemical and enzymatic hydrolysates of β-lactoglobulin: Characterization of the peptides adsorbed at the interface. *Nahrung-Food, 44*(2), 89–95. https://doi.org/10.1002/(sici)1521-3803(20000301)44:2<89::aid-food89>3.3.co;2-l

Rühs, P. A., Affolter, C., Windhab, E. J., & Fischer, P. (2013). Shear and dilatational linear and nonlinear subphase controlled interfacial rheology of β-lactoglobulin fibrils and their derivatives. *Journal of Rheology, 57*(3), 1003–1022. https://doi.org/10.1122/1.4802051

Schram, L. B., Nielsen, C. J., Porsgaard, T., Nielsen, N. S., Holm, R., & Mu, H. (2007). Food matrices affect the bioavailability of (n - 3) polyunsaturated fatty acids in a single meal study in humans. *Food Research International, 40*(8), 1062–1068. https://doi.org/10.1016/j.foodres.2007.06.005

Schröder, A., Berton-Carabin, C., Venema, P., & Cornacchia, L. (2017). Interfacial properties of whey protein and whey protein hydrolysates and their influence on O/W emulsion stability. *Food Hydrocolloids, 73*, 129–140. https://doi.org/10.1016/j.foodhyd.2017.06.001

Shahidi, F. (2015). Omega-3 fatty acids and marine oils in cardiovascular and general health: A critical overview of controversies and realities. *Journal of Functional Foods, 19*, 797–800. https://doi.org/10.1016/j.jff.2015.09.038

Shahidi, F., & Ambigaipalan, P. (2018). Omega-3 polyunsaturated fatty acids and their health benefits. *Annual Review of Food Science and Technology, 9*(January), 345–381. https://doi.org/10.1146/annurev-food-111317-095850

Stupin, A., Rasic, L., Anita, M., Marko, S., & Zlata, K. (2018). Omega-3 polyunsaturated fatty acids enriched hen eggs consumption enhances microvascular reactivity in

Young healthy individuals ana Stupin. *Applied Physiology Nutrition and Metabolism*, 1–32.

Tamm, F., Gies, K., Diekmann, S., Serfert, Y., Strunskus, T., Brodkorb, A., et al. (2015). Whey protein hydrolysates reduce autoxidation in microencapsulated long chain polyunsaturated fatty acids. *European Journal of Lipid Science and Technology, 117* (12), 1960–1970. https://doi.org/10.1002/ejlt.201400574

Tippel, J., Böttcher, S., & Drusch, S. (2016). Determination of the critical micelle concentration of Quillaja saponin. 1–4.

Torcello-Gómez, A., Maldonado-Valderrama, J., Jódar-Reyes, A. B., & Foster, T. J. (2013). Interactions between Pluronics (F127 and F68) and bile salts (NaTDC) in the aqueous phase and the interface of oil-in-water emulsions. *Langmuir, 29*(8), 2520–2529. https://doi.org/10.1021/la3044335

Vivar-Sierra, A., Araiza-Macías, M. J., Hernández-Contreras, J. P., Vergara-Castañeda, A., Ramírez-Vélez, G., Pinto-Almazán, R., et al. (2021). In silico study of polyunsaturated fatty acids as potential SARS-CoV-2 spike protein closed conformation stabilizers: Epidemiological and computational approaches. *Molecules, 26*(3). https://doi.org/10.3390/molecules26030711

Weill, P., Plissonneau, C., Legrand, P., Rioux, V., & Thibault, R. (2020). May omega-3 fatty acid dietary supplementation help reduce severe complications in Covid-19 patients? *Biochimie, 179*, 275–280. https://doi.org/10.1016/j.biochi.2020.09.003